Single particle tracking

Analysis of diffusion and flow in two-dimensional systems

Hong Qian,* Michael P. Sheetz,‡ and Elliot L. Elson*

*Department of Biochemistry and Molecular Biophysics, and ‡Department of Cell Biology and Physiology, Division of Biology and Biomedical Sciences, Washington University School of Medicine, St. Louis, Missouri 63110 USA

ABSTRACT Analysis of the trajectories of small particles at high spatial and temporal resolution using video enhanced contrast microscopy provides a powerful approach to characterizing the mechanisms of particle motion in living cells and in other systems. We present here the theoretical basis for the analysis of these trajectories for particles undergoing random diffusion and/or systematic transport at uniform velocity in two-dimensional systems. The single particle tracking method, based on observations of the trajectories of individual particles, is compared with methods that characterize the motions of a large collection of particles such as fluorescence photobleaching recovery. Determination of diffusion coefficients or transport velocities either from correlation of positions or of velocities of the particles is discussed. A result of practical importance is an analysis of the dependence of the expected statistical uncertainty of these determinations on the number of position measurements. This provides a way of judging the accuracy of the diffusion coefficients and transport velocities obtained using this approach.

INTRODUCTION

The diffusion and systematic drift of membrane proteins has been studied for a number of years for clues to the mechanisms of various cellular processes such as the formation of specialized surface structures (e.g., Dubinsky et al., 1989, and references cited therein), the interactions between membrane bound enzymes and other reaction constituents (e.g., Chazotte and Hackenbrock, 1989), the ligand-receptor-mediated triggering of cellular responses (Schlessinger, 1986), and cellular locomotion (Sheetz et al., 1989). Although the diffusion of membrane proteins may not limit the rates of these processes (e.g., McCloskey and Poo, 1986), measurements of membrane protein mobility can provide important information about membrane structure, interactions between membrane components, and mechanisms of membrane and/or cytoskeleton functions (e.g., Cherry, 1979; Sheetz, 1983; Yechiel and Edidin, 1987; Angelides et al., 1988; Ryan et al., 1988; Duband et al., 1988). During the past two decades most experimental measurements of the lateral diffusion of membrane lipids and proteins have been carried out by fluorescence photobleaching recovery (FPR, e.g., Elson, 1985, and references cited therein), although other methods such as electromigration and postfield relaxation, and diffusion limited excimer formation (Poo, 1981; Eisinger et al., 1986) have also been used. Recently, an optical method has been developed for measuring the movements of single small particles (Geerts et al., 1987) with the possibility of nanometer-scale precision (Gelles et al., 1988; Sheetz et al., 1989). The single particle tracking (SPT) method can provide information not available to FPR and other measurements which are based on the behavior of large ensembles of molecules (Dembo and Harris, 1981). This paper presents methods for analyzing SPT measurements, a comparison of SPT with FPR, and, most important, a consideration of the statistical accuracy of SPT measurements. A similar approach has also been used to characterize the movements on fibroblasts of single LDL receptors monitored by fluorescence video microscopy (Gross and Webb, 1988).

FPR and SPT differ in their spatial resolution and statistical characteristics. FPR measures fluorescence recovery in a photobleached region of the sample due to the diffusion or drift of a large number of molecules. The spatial resolution, limited by the minimum size of a diffraction-limited laser beam, can be on the order of ~ 0.5 μm. SPT measurements provide the x and y coordinates of the centers of individual small (e.g., 40 nm) gold particles, presumed to be rigidly attached to membrane proteins by antibodies or other ligands, recorded at successive times by video enhanced differential interference contrast (DIC) microscopy. The trajectories of random movement of these particles can be determined to a resolution of ≤ 10 nm by analysis of the video images (Gelles et al., 1988; de Brabander et al., 1988). In principle, therefore, SPT can observe motion over a spatial range at least an order of magnitude

Dr. Qian's current address is Institute of Molecular Biology, University of Oregon, Eugene, Oregon 97403-1229.

Dr. Sheetz's current address is Department of Cell Biology, Duke University Medical Center, Box 3011, Durham North Carolina 27710.

0006-3495/91/10/910/12 $2.00

smaller than that accessible to FPR. In an SPT measurement, numerous observations of the stochastic motion of the individual gold particles must be characterized statistically to yield the appropriate time averaged transport properties. In contrast, the participation of many fluorescent particles provides an ensemble average of their diffusion behavior, and therefore their diffusion coefficient, in a single FPR recovery measurement.

The characteristics of the particle motion can be derived either from the trajectory, the sequence of positions: $r_1, r_2, r_3, \ldots$ at times $t_1, t_2, t_3, \ldots$, or from the changes of position at successive times, the velocities: $v_1 = (r_2 - r_1)/\Delta T, v_2 = (r_3 - r_2)/\Delta T, \ldots$ where ΔT is the time interval between each measurement. These two approaches provide the same information about the phenomenological characteristics of particle motion, but from different perspectives. This will be demonstrated along with some mathematical relationships between the two types of analyses. The velocity analysis provides a consistency check on the analysis of trajectories.

MACROSCOPIC AND MICROSCOPIC MEASUREMENTS

For a uniform population of molecules, measurements of the time averaged motion of a single molecule and of the ensemble averaged motion of a collection of independent molecules should yield identical values of the diffusion coefficient or drift velocity (Landau and Lifshitz, 1969). In most systems of biological interest, however, molecules of a specific type can exist in different dynamic states. For example, the Con A receptors bound to 40-nm gold particles on the surfaces both of macrophages (Sheetz et al., 1989) and of fish epidermal keratocytes (Kucik et al., 1989) can be either randomly diffusing or systematically transported toward or away from the cell nucleus. Even though each Con A receptor eventually experiences both states, individual molecules can be seen to be in either the diffusing or the active transport state over a time range of $\sim$10 s. Because at any one time the actively transported molecules represent only a small minority, they cannot be observed by FPR, which measures an averaged behavior of the entire population. In contrast, as long as particles are observed in sufficient numbers to yield an adequate representation of both populations, quantitatively analyzed SPT measurements can clearly characterize the different dynamic properties of the two classes of Con A receptors, as previously demonstrated (Sheetz et al., 1989).

The superior spatial resolution of SPT over FPR ($\sim$10 nm vs. $\sim$0.5 μm) is even more useful in studying systems which impose highly localized constraints on the motion under study. In principle, high spatial (or temporal) resolution is not required to measure the diffusion coefficient for a simple diffusion process in an unlimited space. If one waits long enough, sufficient diffusion will occur to permit adequate measurement, even using an instrument with very low spatial (or temporal) resolution. Biological systems, however, frequently impose spatial constraints on particle motion. For example, it has been observed that the diffusion of cell surface membrane proteins is retarded by unknown forces and/or structures. One structural model proposes that the membrane proteins are confined to cytoskeletal "corrals" which permit free movement within the corral but retard passage from one corral to the next (Sheetz, 1983). Therefore, submicron spatial resolution is necessary to detect the motion within the corral, and such resolution is accessible to SPT but not to FPR.

Constraint of the range of particle motion, however, also imposes demands on the temporal resolution required for the measurement. When a characteristic distance is set either by the measurement method or by the structure of the sample system, a characteristic time consequently arises together with a corresponding requirement for sufficient temporal resolution to observe the dynamic process within this time. For surface diffusion with diffusion coefficient, D, the characteristic time, Δt_c, is related to the characteristic distance Δx_c as $\Delta t_c \sim \Delta x_c^2/4D$. A decrease in the characteristic distance causes a corresponding decrease in the characteristic time and so may require a corresponding increase in the temporal resolution of measurement. Similarly, a shortening of the characteristic time causes a decrease in characteristic distance and so an increase in the spatial resolution of the measurement is necessary. For example, in a measurement of fast diffusion of a protein in solution by FPR, one often uses a large illuminated volume to increase the characteristic diffusion time above the temporal resolution limit of instrument. Conversely, the characteristic FPR diffusion time for a membrane protein with diffusion coefficient $\sim 10^{-9}$ cm^2/s in a small cytoskeletal corral (0.1 $\sim$ 0.3 μm, Sheetz, 1983) should be $\sim$100 ms. This should be accessible to FPR, which is capable of measurements of processes with characteristic times $\geq$100 μs. Nevertheless, the spatial resolution of FPR, determined by the diffraction limited beam radius ($\geq \sim$0.5 μm), is insufficient. In contrast the 10-nm spatial resolution of SPT is sufficient to measure diffusion within a corral, but standard video methods have insufficient temporal resolution ($\sim$30 ms). Therefore, sufficient spatial and temporal resolution are both needed to measure a restricted diffusion. The temporal resolution of video microscopy can, however, be improved by photoelectric techniques to the range of 100 μs (Howard and Hudspeth, 1987; Kamimura, 1989),

presumably sufficient to measure the diffusion of a particle with diffusion coefficient $D = 10^{-8}$ cm^2/s in a 100-nm cage.

SPT and FPR also differ in that the former characterizes microscopic properties of diffusing particles, namely, the transition probabilities, i.e., the probability that a particle initially at position r' will be found at r at a later time t. In many cases, the steady state microscopic distribution does not affect the outcome of the measurement. This is quite different from FPR measurements in which the steady-state distribution usually is important in the overall results (see below).

MEAN SQUARE DISPLACEMENT AND CORRELATION FUNCTION OF POSITION

SPT yields the trajectory $r(t) = [x(t), y(t)]$, i.e., the coordinates at each time t, of a particle undergoing two-dimensional diffusion and/or systematic transport. Because the data are stochastic, they must be analyzed statistically to yield the conventional phenomenological diffusion coefficient and drift rate (Chandrasekhar, 1943). The mean square displacement (MSD) of the trajectory, denoted as $\rho(t)$, is a convenient quantitative characteristic of the motion:

$$\rho(t) = \langle [r(t) - r(0)]^2 \rangle = \int\int P(r')(r - r')^2 P(r|r', t)\, dr dr'. \quad (1)$$

Here, $P(r)$ is the steady-state distribution of particle position and $P(r|r', t)$ is the transition probability, i.e., the probability that a particle originally at r' will be at r after a time period t. Because the process is stationary, the ensemble average can be computed as a time average for a single trajectory (Landau and Lifshitz, 1969). Therefore,

$$\rho(t) = \int |r(t + t') - r(t')|^2\, dt'.$$

This allows determination of $\rho(t)$ from an experimentally measured trajectory. Particle positions are recorded in the form of a time sequence $[x_n = x(n\Delta T), y_n = y(n\Delta T) | n = 0, 1, 2, \ldots]$, with the data acquisition time interval ΔT. Therefore $\rho(t)$ and its x, y components are expressed in terms of discrete time sequences:

$$\rho_x(n\Delta T) = \sum_{i=0}^{N} (x_{i+n} - x_i)^2/(N + 1)$$

$$\rho_y(n\Delta T) = \sum_{i=0}^{N} (y_{i+n} - y_i)^2/(N + 1), \quad (2)$$

and

$$\rho_n = \rho(n\Delta T) = \rho_x(n\Delta T) + \rho_y(n\Delta T). \quad (3)$$

Fig. 1 depicts $\rho(t)$ for simple diffusion.

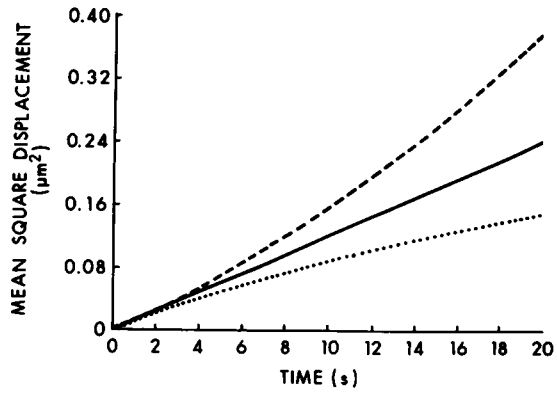

FIGURE 1 The mean square displacement as function of time for a diffusing particle. (——) pure diffusion; (-----) diffusion with flow; (· · ·) diffusion in a cage. For these calculations $D = 3 \times 10^{-11}$ cm^2/s, $V = 0.02$ μm/s, and the cage size was 1 μm × 1 μm. The $\rho(t)$ for diffusion in a cage was calculated as described by Kolinski et al. (1986), using their Eq. 5 extended to a two-dimensional system.

The mean square displacement as function of time is closely related to the position correlation function:

$$g_r(t) = \langle r(t)r(0) \rangle = \int\int rr'P(r')P(r|r', t)\, dr dr' = (1/2)\int\int [r^2 + r'^2 - (r - r')^2]P(r')P(r|r', t)\, dr dr' = \langle r^2 \rangle - \rho(t)/2. \quad (4)$$

Time correlation functions have been widely used in kinetic studies (Zwanzig, 1965). Eq. 4 provides a formal link to other methods used to measure diffusion such as fluorescence correlation spectroscopy (FCS), a technique similar to FPR (Elson, 1985), and dynamic light scattering (DLS). In these techniques it is not the position of the diffusing particle itself as a stochastic process $r(t)$, but rather some function of the particle positions $I(r)$, that can be directly measured. The desired kinetic information is extracted from the time correlation of the process $I[r(t)]$. In FCS, $I(r) = I_0 \exp(-r^2/\omega_0^2)$, is the Gaussian laser profile which excites fluorescence from particles at positions r. Then the e^{-2} radius ω_0 determines the characteristic distance for this measurement. In dynamic light scattering: $I(r) = \exp(ir \cdot q)$ where q is scattering vector, which varies inversely as the wavelength of the incident light, and $1/|q|$ is the characteristic distance imposed on the diffusion measurement (Cummins et al., 1969). In both cases, the photocurrent $i(t) \propto I[r(t)]$ is the directly measured quantity.

Simple diffusion

The coordinates $r = (x, y)$ of a particle undergoing free diffusion can be represented as a Gaussian process with

transition probability (Chandrasekhar, 1943):

$$P(r|r', t) = (1/4\pi Dt) \exp[-(r - r')^2/4Dt]. \quad (5)$$

This transition probability for free space is applicable so long as the characteristic dimension of the space available for diffusion, L, is sufficiently large that the measurement time interval is much smaller than $L^2/4D$. Then $\rho(t) = \langle[r(t) - r(0)]^2\rangle = 4Dt$. The average $\langle \cdots \rangle$ is taken not only over all the possible trajectories but also over all the initial positions $r(0)$. This emphasis, although unnecessary for free diffusion, is crucial to account for the effects of the boundaries in an analysis of diffusion within a finite region.

For diffusion in a finite region, from Eq. 4, $\rho(\infty) = 2(\langle r^2\rangle - \langle r\rangle^2)$, which is proportional to the size of the region accessible for diffusion. For example, $\rho(\infty) = R^2$ for a disk with radius R; $\rho(\infty) = \lambda^2/3$ for a square of $\lambda \times \lambda$. (More precisely, $\sqrt{\rho_x(\infty)}$ and $\sqrt{\rho_y(\infty)}$ specify the linear dimensions of the accessible region). Therefore, a measurement of $\rho(\infty)$ yields an estimate of the finite area accessible for diffusion. For free diffusion, of course, the available area is infinite, and so $\rho(t)$ increases without bound, i.e., both $\rho(\infty)$ and the second moment $\langle r^2\rangle = \infty$. Hence, the time correlation function $\langle r(t)r(0)\rangle$ does not exist for free diffusion, but its difference from $\langle r^2\rangle$, that is the $\rho(t)$, does exist. A typical plot of $\rho(t)$ versus t for diffusion in a finite region is also shown in Fig. 1.

Diffusion with flow

When diffusion and drift or flow with constant velocity V are superimposed, the transition probability becomes $P(r|r', t) = (4\pi Dt)^{-1} \exp[-(r - r' - Vt)^2/4Dt]$ (Chandrasekhar, 1943). Therefore,

$$\rho(t) = 4Dt + V^2t^2 \quad (6)$$

Here we have again supposed that the total measurement time is much smaller than $L^2/4D$. For most cell experiments, $L \sim 10$ μm and $D \sim 10^{-10}$ cm^2/s, therefore $L^2/4D > 10^3$ s.

When there is drift or flow, $\rho(t)$ is no longer linear in time but, as shown in Eq. 6, has positive curvature. In contrast to simple diffusion for which the slope, $\rho'(t) = d\rho(t)/dt = 4D$, is a constant, when drift or flow contributes, $\rho'(t)$ continually increases ($\rho''(t) = 2V^2 > 0$) as if the diffusion rate for a particle were faster the farther it had moved. This indicates that the contribution of systematic motion becomes dominant at longer times. Even if flow or drift is slow compared to diffusion, because of its dependence on t^2, the second term in Eq. 6 must dominate $\rho(t)$ at longer times. Hence, when both diffusion and flow are present, the former will tend to dominate at early times ($t \ll 4D/V^2$), the latter, at later times ($t \gg 4D/V^2$). If there are no active contributions to the motion, either $\rho''(t) = 0$ for simple diffusion or $\rho''(t) < 0$. As shown below, the latter possibility could occur if there were barriers which slowed the diffusion rate beyond some characteristic spatial scale (cf Fig. 1). A curve-fitting procedure can be used to estimate both D and V from experimentally determined $\rho(t)$ (cf Sheetz et al., 1989).

Nonideal diffusion due to interactions

Negative curvature of $\rho(t)$ indicates that diffusion occurs not as a simple homogeneous process in free space but rather that its rate is lower over longer than over shorter distances. This observed behavior is most simply interpreted in terms of interactions between the diffusing particles and other mobile or immobile structures. Nonideal diffusive behavior has been studied theoretically recently either using Monte Carlo methods (Saxton, 1987, 1989, 1990) or by analysis of a two-dimensional version of a generalized Smoluchowski Equation (Abney et al., 1989). The results of these studies indicate that the effects of interactions, either attractive or repulsive, with either mobile or immobile obstacles is to retard the rate of diffusion. Furthermore, the behavior of $\rho(t)$ will depend on the concentration of the obstacles. Suppose that the barriers are separated from one another by a mean characteristic distance Λ. On a spatial scale much smaller than Λ the rate of diffusion is not affected by the barriers, and so the diffusant is characterized by a localized diffusion coefficient D_m. On a larger spatial scale, however, the presence of the barriers will reduce the diffusion coefficient. Therefore, with sufficient spatial and temporal resolution, $\rho(t)$ should show a fast phase due to the local diffusion of the particle with an initial slope of $4D_m$. This measurement requires both spatial and temporal resolution sufficient to measure motion over distances small compared to Λ, and times short compared to $\Lambda^2/4D_m$. On a longer time scale and therefore a larger spatial scale $\rho(t)$ increases more slowly with time to define an effective diffusion coefficient, D_M, which is diminished due to the interactions of the diffusant with the barriers and depends on the fraction of the surface covered by barriers (Saxton, 1989). Percolation theory indicates that long-range diffusion will cease altogether (i.e., $D_M \to 0$) if the barriers are immobile and cover more than a threshold fraction of the surface. Also, the long-time behavior of $\rho(t)$ might depend nonlinearly on t in the presence of immobile obstacles (cf Ghosh and Webb, 1990). For immobile barriers below the critical threshold and for mobile barriers at any fractional coverage of the surface the rate of long range diffusion will be greater than zero, although diminished relative to diffusion unimpeded by

barriers. Due to the high concentration of interacting proteins and other possible barriers in membranes the observed behavior of $\rho(t)$ will be dominated by the latter phase in which diffusion is obstructed by interactions (Sheetz et al., 1989; Ghosh and Webb, 1990), and this will be our principal concern.

FPR FOR STEADY STATE DIFFUSION WITH DRIFT

A comparison of SPT and FPR for the characterization of systems in which particles both diffuse and systematically drift shows an important difference in the applicability of the two methods. In a system in which all fluorophores are simultaneously undergoing both systematic drift with velocity V and diffusion with diffusion coefficient D the FPR recovery, restricted to small extents of photobleaching for simplicity, is (Magde et al., 1978):

$$f(t) = 1 - \kappa \exp\{-(t/\tau_f)^2/(1 + t/\tau_d)\}/(1 + t/\tau_d). \quad (7)$$

Here, κ describes the extent of bleaching, $\tau_d = \omega_0^2/4D$ and $\tau_f = \omega_0/V$. This recovery, when $t \ll \tau_d$, is similar to that for uniform flow without diffusion:

$$f(t) \simeq 1 - \kappa \exp\{-(t/\tau_f)^2\}. \quad (8)$$

When the effects of systematic drift are just compensated by diffusion, however, a steady-state concentration gradient is established; there is no macroscopic mass transfer. Then, $P(r) \sim \exp(V \cdot r/D)$ (Bretscher, 1976). Under these conditions, the FPR fluorescence recovery $f(t)$ after a minimal extent of photobleaching has the form:

$$f(t) \simeq 1 - \kappa \exp(-\tau_d t/\tau_f^2)/(1 + t/\tau_d). \quad (9)$$

(This result can be obtained either by calculation of the FPR recovery in the steady-state gradient or from the above more general expression for $f(t)$ by setting $t \gg \tau_d$. This correspondence is expected because in the long time limit, the equilibrium distribution $\exp(V \cdot r/D)$ would have been established.) Therefore, the sensitivity of FPR measurements to flow in the presence of diffusion is determined by the ratio of the characteristic times for diffusion and flow, τ_f/τ_d. For a typical cell, $V \simeq 0.01$ μm/s, $D \simeq 10^{-10}$ cm^2/s, and in typical experiments, $\omega_0 \simeq 1$ μm, therefore, $\tau_d \simeq 25$ s, $\tau_f \simeq 100$ s. In Fig. 2, to emphasize the difference between simple diffusion and diffusion plus drift, the reciprocal of FPR recovery curves are plotted. A straight line is expected for simple diffusion in this type of plot. These curves show that even for a uniform population of particles which diffuse and flow simultaneously, the effect of flow is barely

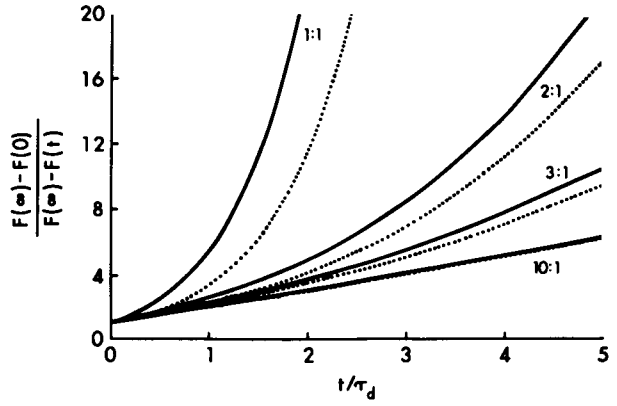

FIGURE 2 Effect of flow on the FPR recovery curve. The fluorescence recovery, $f(t)$, is plotted in reciprocal normalized form: $1/[1 - f(t)]$. The ratio τ_f/τ_d is presented for each pair of curves. (———) recovery after photobleaching a steady state concentration gradient resulting from a balance between flow and diffusion yielding $P(x) = \exp(V \cdot r/D)$. (· · · · ·) recovery after photobleaching an initially uniform concentration, $P(x) = 1$.

evident with this ratio of diffusion and flow rates. Within limits, τ_d/τ_f can be increased and so the ability to detect flow can be enhanced by increasing the beam radius, ω_0, using a microscope objective lens of lower magnification. SPT measurements over long enough time, however, will always detect systematic drift (cf Fig. 1). Theoretically, FPR measurements extended to $t \gg \tau_d$ could detect even a small drift as a deviation from a straight line plot as in Fig. 2. This is difficult, however, because of uncertainty in determining the final extent of recovery, $F(\infty)$, (van Zoelen et al., 1983).

DATA ANALYSIS IN VELOCITY SPACE

The velocity autocorrelation function $g_v(t) = \langle v(t)v(0)\rangle$ can supply an explicit test that the observed particle motion is behaving as simple diffusion. According to the rigorous mathematical theory of ideal diffusion, which neglects all the detailed underlying mechanism of motion, $g_v(t)$ should behave as a Dirac delta function: $\langle v(t)v(0)\rangle = 2D\delta(t)$ (Zwanzig, 1965). For our purposes, this relationship results from the fact that the velocity $v(t)$ is averaged over a time interval ΔT (ms) which is long compared to the time between intermolecular collisions ($< 10^{-12}$ s). Because of the large number of collisions during the measuring interval the velocities determined for successive intervals are completely uncorrelated (cf Chandrasekhar, 1943). Then, if the particle is undergoing simple diffusion (with or without drift), a computation of the correlation function from the experi-

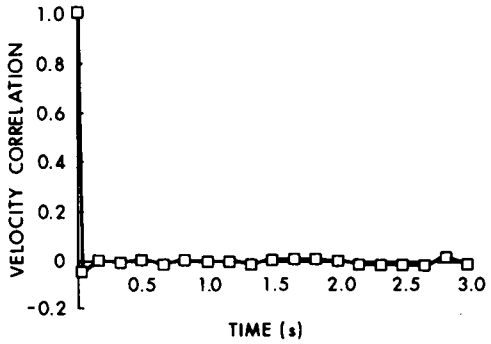

FIGURE 3 The time correlation $\langle \Delta v(t) \Delta v(0) \rangle$ calculated from experimental measurements of a diffusing 40-nm gold bead bound by the plant lectin Concanavalin A to the surface of a mouse macrophage (Sheetz et al., 1989). This figure illustrates the expected delta function character of the velocity correlation function.

mental measurements as $g_v(n\Delta T) = \Sigma_{i=1}^{N} (v_{i+n} v_i)/N$ ($n = 0, 1, 2, \ldots$.) should have a nonzero value for $n = 0$. Fig. 3 demonstrates that this condition is fulfilled for our experimental measurements.[1] Nevertheless, it is still possible that particles apparently undergoing random motion might be driven by forces other than thermal molecular collisions. For example, particles on a cell surface might be driven in random directions by cytoskeletal motors or by the inhomogeneity of the cortical cytoskeletal network. If the duration of a "step" in these processes were sufficiently great, a computation of $g_v(t)$ might show that the particle motion deviated from simple diffusion; on the other hand, if the duration of these "steps" were small compared to the measurement resolution, the motion would be sufficiently characterized by a simple diffusion model (cf Nossal, 1971). Measurement methods with higher temporal resolution than 30 ms are now available which could yield more information about the mechanism of nonBrownian particle motion. In principle, even in the absence of active transport processes, the presence of obstacles to diffusion could impose a significant correlation on particle trajectories and thereby invalidate the delta function relationship given above. As shown by Fig. 3 this does not appear to have happened in measurements at the current level of spatial and temporal resolution.

Under typical circumstances the diffusion coefficient can be calculated from $\langle v^2 \rangle$. The measurement of $v = \Delta x/\Delta T$ is limited by ΔT, the single video image acquisition time interval. Then, because ΔT is fixed,

$$\begin{aligned} \langle v^2 \rangle &= \langle (\Delta r/\Delta T)^2 \rangle \\ &= \langle \Delta r^2 \rangle / (\Delta T)^2 \\ &= 4D/\Delta T. \end{aligned} \tag{10}$$

If both diffusion (D) and drift (V) are considered,

$$\begin{aligned} \langle \Delta r^2 \rangle &= 4D\Delta T + (V\Delta T)^2 \\ \langle v^2 \rangle &= 4D/\Delta T + \langle v \rangle^2 \\ \langle (\Delta v)^2 \rangle &= \langle v^2 \rangle - \langle v \rangle^2 = 4D/\Delta T. \end{aligned} \tag{11}$$

Hence, $\langle (\Delta v)^2 \rangle \Delta T/4$ yields the diffusion constant D (Fig. 4). For a system involving drift, obviously $\langle v \rangle$ is another measure of the drift rate. The calculation of $\langle v \rangle$ and $\langle (\Delta v)^2 \rangle$ (the first two moments of the velocity histrogram) provide an estimate for the same D and V as polynominal fitting of $\rho(t)$ to $V^2t^2 + 4Dt$. As expected, there exists a relationship between the experimentally determined $g_v(t)$ and $\rho(t)$, in fact $2g_v(t) = \rho''(t)$, as shown in Appendix A.

STATISTICAL ACCURACY IN DIFFUSION MEASUREMENTS

Because diffusion is a stochastic process and the correlation calculation we have presented is statistical, even with infinitely precise measurements of positions the calculated mean square displacement (MSD), and the diffusion coefficient and drift rate derived therefrom, will have theoretically expected statistical variances.

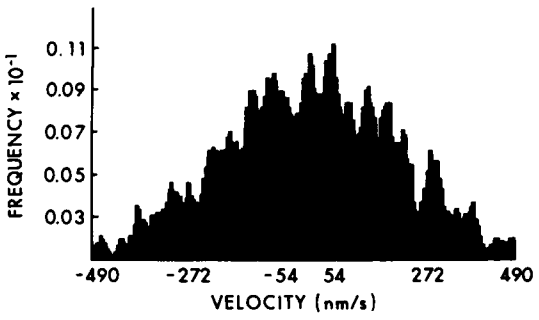

FIGURE 4 The histogram of velocity in a typical experimental measurement of a diffusing 40-nm gold bead bound by Concanavalin A to the surface of a mouse macrophage as in Sheetz et al. (1989). For this measurement $\Delta T = 0.033$ s. The histogram yields $\langle v \rangle = 58.3$ nm/s and $\langle \Delta v \Delta v \rangle = 8.18 \times 10^5$ (nm/s)^2, therefore, $D = 1.3 \times 10^{-10}$ cm^2, calculated from $\langle (\Delta v) \rangle^2 = 2D/\Delta T$. (Here we are considering the component of diffusion along only one axis, and so we treat the diffusion as one-dimensional.)

[1]The time integral of $g_v(t)$ provides the diffusion coefficient according to the equation $2D = \int \langle v(t)v(0) \rangle dt$. If $v(t)$ is the instantaneous velocity of the particle, the integral takes into account its detailed dynamics over a period which allows many collisions but not substantial displacement. If, however, averaged velocities are used then the delta function relationship indicated above renders this equation trivially correct.

Therefore, an estimate of statistical accuracy is essential for our analysis.

The variance arises from the stochastic nature of diffusion. Within the limits of the accuracy of the experimental measurements of particle positions, this variance will diminish as the number of position measurements increases.

We can begin a statistical analysis by supposing that we have K independent measurements of the squared displacement, $\xi = |r(t) - r_0|^2$. We want to calculate the variance of the mean $\bar{\xi} = \{\xi(1) + \xi(2) + \cdots + \xi(K)\}/K$. First, let us consider a pure diffusion problem. The probability distribution of ξ considered as a random variable is

$$\text{Prob}\{z \le \xi \le z + dz\} = (1/4Dt)\ \exp(-z/4Dt)\ dz \qquad z > 0. \quad (12)$$

From this, as pointed out in Appendix B, we can obtain the probability distribution of $\bar{\xi}$ for which the variance is $(4Dt)^2/K$. The measurement at time intervals ΔT of N consecutive positions r allows the calculation of ρ_n $[=\rho(n\Delta T)]$, the experimentally determined mean square displacement for a time interval nΔT by averaging over $N-n+1$ measurements, i.e., 0 to n, 1 to $n+1$, 2 to $n+2, \ldots, N-n$ to N. Successive determinations are not statistically independent, however, due to the overlap between the measurements. Taking account of this dependence, the expected variance for the calculated ρ_n would be larger (see Eq. B5, Appendix B, setting $K = N - n + 1$, and noting $(2n^2 + 1)/3n \ge 1$):

$$(4Dn\Delta T)^2\,(2n^2 + 1)/3n(N - n + 1). \quad (13)$$

The variance increases with increasing n. This is because the larger n, the smaller will be the number of statistically independent samples of displacement within the interval $N\Delta T$. Hence the maximum value of n (the last point calculated in the MSD), say $n = m$, will incur the largest statistical uncertainty. For $n = m$ the standard deviation is less than $4Dm\Delta T[2m/3(N - m + 1)]^{1/2}$ (Fig. 5). Therefore, even in the worst case, the standard deviation in $\rho(t)$, $0 \le t \le m\Delta T$, is less than $4Dm\Delta T[2m/3(N - m + 1)]^{1/2}$. Taking the maximum uncertainty of this last, mth, data point, ρ_m, as an upper bound yields an estimated relative error in the slope of $\rho(t)$ and therefore also in D of $\sim \pm[2m/3(N - m)]^{1/2}$. If $3(N - m)/2m$ is chosen to be >100, then the expected error in the diffusion constant due to stochastic uncertainty is smaller than 10%.

Whereas the diffusion coefficient is estimated from the slope, the rate of systematic transport or drift is determined from the curvature of $\rho(t)$. The statistical uncertainty in $\rho(t)$ due to the stochastic character of diffusion also leads to uncertainty in the estimation of the drift rate. An upper bound of the uncertainty in the curvature of $\rho(t)$ can be obtained by considering only three points in ρ_n, $n = 0, 1, m$, where the relative uncertainties are $0, \pm 1/\sqrt{N}$ and $\pm[2m/3(N - m)]^{1/2}$, respectively. To obtain an upper bound of the curvature likely to be observed for a randomly diffusing particle, we use an underestimation of $\rho(1) = 4D\Delta T(1 - 1/\sqrt{N})$, an overestimation of $\rho(m) = 4Dm\Delta T[1 + (2m/3(N - m))^{1/2}]$, together with $\rho(0) = 0$ to maximize the curvature calculation. It should be possible to detect true systematic transport with a velocity, V, comparable to this curvature. Therefore:

$$(Vm\Delta T)^2 = 4Dm\Delta T[[2m/3(N - m)]^{1/2} + 1/\sqrt{N}] \le 4Dm\Delta T[m/(N - m)]^{1/2} \quad (14)$$

Hence, an error in estimating the drift rate should be $< 2[D^2/[m(N - m)(\Delta T)^2]]^{1/4}$. For example, with $N\Delta T = 100$ s, $D = 10^{-12}$cm^2/s, and $m\Delta T = 50$s, a drift rate as small as 3nm/s should be detectable, and for $D = 10^{-10}$cm^2/s, drift on the order of 30 nm/s would be detectable.

Similar statistical considerations hold for determination of rates of diffusion or systematic transport from velocity measurements. Experimental estimates of $\langle v \rangle$ and $\langle \Delta v \Delta v \rangle$ are obtained from the measured histogram of velocity as $\bar{v} = (v_1 + v_2 + \cdots v_N)/N$ and $\overline{v^2} = (v_1^2 + v_2^2 + \cdots v_N^2 v)/N$, respectively, where N is the total number of data points acquired. One may verify that $\langle v \rangle = \langle (r_N - r_0) \rangle/(N\Delta T)$ and $\langle v^2 \rangle = \rho_1/\Delta T^2$. Therefore, $\overline{v^2}$ yields a diffusion coefficient valid only on the time scale of ΔT, i.e., the experimental initial slope of $\rho(t)$. By definition $v^2 = (\Delta r/\Delta T)^2$, hence the distribution of v^2 corresponds to that of Δr^2. Moreover, knowing the probability distribution of Δr^2 and observing that $\langle (\Delta r)^2 \rangle/4D\Delta T = \langle v^2 \rangle \Delta T/$

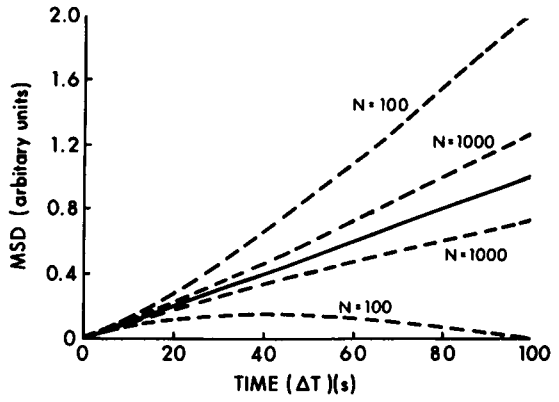

FIGURE 5 The relative statistical error in msd, $\rho(t)$ (——). Upper and lower curve are $\langle \rho_n \rangle \pm (\langle \Delta\rho_n \Delta\rho_n \rangle)^{1/2}$. N is the total number of position measurements.

$4D$, we can use the method of Appendix B to obtain the probability distribution of v^2 from a series of N independent measurements:

$$\begin{aligned}&\text{Prob}\{z \le \overline{v^2}\Delta T/4D \le z + dz\}\\&= \text{Prob}\{z \le \rho_1/4D\Delta T \le z + dz\}\\&= N^N z^{N-1}/(N-1)!\exp(-Nz)dz. \qquad (15)\end{aligned}$$

The probability to obtain the correct diffusion coefficient from $\overline{v^2}$, within 10% error, can be calculated by integrating the above distribution as follows:

$$\begin{aligned}&\text{Prob}\{|\overline{v^2}\Delta T - 4D|/4D < 0.1\}\\&= \text{Prob}\{|\overline{v^2}\Delta T/4D - 1| < 0.1\}\\&= \text{Prob}\{0.9 \le \overline{v^2}\Delta T/4D \le 1.1\}\\&= \int_{0.9}^{1.1} N^N z^{N-1}/(N-1)!\exp(-Nz)\,dz. \qquad (16)\end{aligned}$$

This probability is 68.4% for $N = 100$ and 99.8% with $N = 1{,}000$. The intrinsic statistical accuracy is high for these measurements, but the result might not be the diffusion coefficient we seek, because there may be contributions to the MSD from other kinds of motion. Therefore, it is important to ascertain whether other processes contribute by calculating the full time course of $\rho(t)$, and verifying its linearity.

When $N \to \infty$, for a purely diffusional process $|r_N - r_0| \sim N^{1/2}$, therefore $|\bar{v}| = |r_N - r_0|/N \sim N^{-1/2} \to 0$. In experimental measurements with finite N, however, there is always a finite probability to have $|\bar{v}| > v_0$ (an arbitrary velocity) even in the absence of systematic transport. That is, integrating the probability distribution for v,

$$\begin{aligned}\text{Prob}\{|\bar{v}| > v_0\} &= \text{Prob}\{|r_N - r_0| > Nv_0\}\\&= \exp(-v_0^2 N\Delta T/4D). \qquad (17)\end{aligned}$$

The statistical error in an estimation of drift rate, i.e., the variance in $\bar{v}$, is $\int v_0^2 d[\exp(-v_0^2 N\Delta T/4D)] = 4D/N\Delta T$. Hence, with $N\Delta T = 100$ s, $D = 10^{-12}\text{cm}^2/\text{s}$, the detectability of the drift rate (the square root of the variance) is ~ 2 nm/s. Therefore, at its worst the trajectory method is comparable to the velocity analysis for obtaining the drift rate. This is expected because in the trajectory method, the whole range of time correlation is used (which is the reason that n is involved), while in $\langle v\rangle$ only a single moment is used.

It is also worth noticing that the correlation coefficient for ρ_n $(=\rho(n\Delta T))$ and ρ_m $(=\rho(m\Delta T))$ is n/m, $(m > n)$ (Appendix C). Therefore, ρ_n and ρ_m are highly correlated when $(m - n) \ll n, m$. This means that we should not expect the random deviation in the experimental ρ_n to be symmetrically distributed around $\langle\rho_n\rangle$. In other words, the statistical accuracy of a measurement of $\rho(t)$ cannot be judged from the smoothness of a plot of $\rho(t)$ versus t. Rather, the accuracy of a measurement should be assessed from the reproducibility of a series of corresponding measurements. This distinction has been previously pointed out by Gross and Webb (1988) and has also been verified by computer simulation (Fig. 6).

EFFECT OF ERROR IN POSITION MEASUREMENTS

As demonstrated by Gelles et al. (1988), there is an uncertainty in the measurements of the position of a diffusing particle. The uncertainty is due to measurement error and blurring over the acquisition time of each video frame (~ 30 ms). This uncertainty usually is a random error which is not correlated with time. Therefore, its contribution to the MSD calculation is similar to that of shot noise with amplitude on the order of 25–50 nm^2, and should have no effect on the $\rho(t)$ function other than at zero time. Hence, the errors in position measurement should not influence the time course of the mean squared displacement. Nevertheless, uncertainties due to the stochastic nature of diffusion place limits on the extent to which either positive or negative curvatures

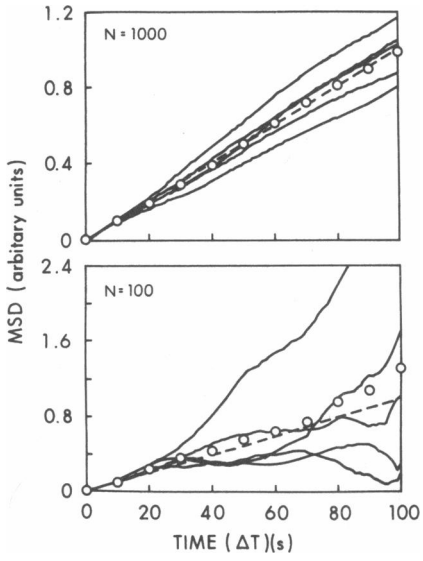

FIGURE 6 Computer simulations for a diffusing particle with the total number of position measurements, $N = 100$ and $N = 1{,}000$. There are five independent simulations for each N. The dashed line is the theoretically expected mean square displacement, and the circles are the averages of the five simulations. Although several of the curves for individual simulations are relatively smooth, the overall standard deviation can be judged not from the smoothness of single curve but must be determined rather by a set of curves.

due, respectively, to systematic transport or to constraints on the range of diffusion can be detected.

DISCUSSION

We have described a simple and convenient method for analyzing the trajectories of individual particles, to obtain the macroscopic diffusion coefficients and drift velocities which characterize their motion. This complements methods such as FPR and FCS which monitor large populations of particles. A major advantage of the SPT method is its ability to characterize the distinct dynamic properties of minority fractions of a population which might be undetectable by FCS or FPR (cf Sheetz et al., 1989). Even for a homogenous population of particles, however, valid SPT measurements require the observation either of a single particle over a long time period or of many particles for shorter times to account adequately for the stochastic character of diffusion. In contrast to FPR both SPT and FCS share the requirement for long observation times which result from the statistical character of the two methods.

The statistical validity and mechanistic interpretation of the measurements are governed by characteristic times determined by the structure of the experimental system and measurement times set by the experimenter. In general, there are two important operational factors in these measurements. The time interval between each position measurement should be smaller than the characteristic time of interest. On the other hand, only those measurements with time interval larger than the characteristic time can be considered statistically independent. Whereas the former point must be considered to provide sufficient temporal resolution of the measurement, the latter point is important in judging experimental accuracy, which increases as the number of statistically independent measurements increases.

When there is only simple unrestricted diffusion, as indicated by the linear dependence of $\rho(t)$ on t, the time resolution of the position measurements does not influence the determination of the diffusion coefficient. This is because $\langle[r(t) - r(0)]^2\rangle \sim t$ (i.e., there is no intrinsic characteristic time in the system, and the correlation between each measurement is negligible). Thus, the duration of a single measurement (ΔT) can in principle be prolonged to any extent necessary to observe sufficient motion, even of very slowly diffusing particles.

In contrast, when diffusion is constrained by barriers or boundaries, an individual microscopic diffusive fluctuation takes place on average over a characteristic correlation time, τ, defined in terms of the distance, Λ, separating the barriers or boundaries: $\tau \sim \Lambda^2/4D$. The determination of the diffusion coefficient from the observation of a brief single diffusive fluctuation, even if performed with high precision, is relatively inaccurate due to the stochastic nature of the diffusion process. To obtain an accurate estimate of the diffusion coefficient many of these microscopic fluctuations must be observed. The accuracy of the measurement increases with the number of the fluctuations observed and therefore with the total time of observations, T. Thus, the relative error varies as the reciprocal of the square root of the number of observed fluctuations and so as $1/(T/\tau)^{1/2}$. Considering again the model of membrane protein diffusion constrained by cytoskeletal corrals (Sheetz, 1983), we can suppose that, $D = 10^{-9}$ cm^2/s and $\Lambda \sim 100$ nm, and so $\tau \sim 25$ ms. Therefore, if the duration of the measurement is 25 s and $\Delta T = 2.5$ ms, 10,000 data points will be obtained and so D should be obtained with an estimated relative error of 1%. Of course, setting $\Delta T = 2.5$ ms assumes a >10-fold faster rate of data acquisition than is available using conventional video methods. To interpret the measurements in terms of free diffusion, it is necessary to confine attention to $\rho(n\Delta T)$ for very small n values. When $n\Delta T$ becomes comparable to τ, the walls of the corrals strongly influence the diffusion behavior of the particles (cf Fig. 1). Even for $n = 2$ or 3, however, it should be possible to determine D from the initial slope of the plot of $\rho(t)$ vs. t. For particles diffusing in a cage the deviation of $\rho(t)$ from the straight line behavior expected for free diffusion provides an estimate of the dimensions of the cage.

This example also demonstrates how in principle SPT could provide a powerful approach for the analysis of interactions between diffusing particles and mobile or immobile obstacles. In fact the measurement of $\rho(t)$ should allow a direct comparison between theory (e.g., Abney et al., 1989; Saxton, 1987) and experiment. In real membranes, however, the distances between structures that could retard diffusion are likely to be quite small. Hence, improvements in spatial and temporal resolution of the measurement methods will be required to achieve the full potential of this approach.

To carry out a complete analysis of the statistical accuracy of SPT measurements in systems in which interactions with mobile or immobile obstacles retard diffusion would require determination of the probability distribution of $\rho(t)$ in the presence of the obstacles. This is beyond the scope of this work. Nevertheless, a more approximate discussion is possible in much simpler terms. In the presence of mobile obstacles or of immobile obstacles below the percolation threshold $\rho(t)$ is proportional to t (Saxton, 1987; Abney et al., 1989). Hence, even in the presence of obstacles it is possible to define a limiting effective diffusion coefficient $D_{eff} = (1/4)d\rho(t)/dt$ for t sufficiently great. It is reasonable to suppose that diffusion is still essentially random under

these circumstances and therefore that $\rho(t)$ still has a Gaussian probability distribution. Then the analysis presented in Appendix B remains approximately valid. Hence, as above, we can estimate the relative error in the value of D measured from the slope $d\rho/dt$ to be about $\pm[2m/3(N-m)]^{1/2}$ where $m\Delta T$ is the largest interval used in the calculation of $\rho(t)$. Because the value of D is decreased due to interactions with the obstacles, a longer time will be required to diffuse a given distance and so a correspondingly longer interval $m\Delta T$ is likely to be selected. This in turn will require a longer total measuring period $N\Delta T$ to achieve the same accuracy as for unimpeded diffusion in the absence of obstacles. A summary of the dependence of $\rho(t)$ on time and of expected relative errors for different mechanisms of transport is presented in Table I.

A practical consideration in studies of the behavior of membrane glycoproteins is the possible perturbation which results from attaching the observable particle. Likely to be most significant is the binding of a number of glycoproteins to a single particle due both to the multivalency of the binding molecules, such as antibodies or lectins, and the presence of several binding molecules on the particle. Likely to be less significant is the drag on the particle as it moves through the extracellular solution of relatively low viscosity. A comparison of diffusion coefficients measured by SPT and FPR is given in Table II.

TABLE I Summary of results

Transport mechanism	$\rho(n\Delta T)$	Expected variance
Free diffusion	$4Dn\Delta T$	$p(4Dn\Delta T)^2$
Free diffusion + flow	$4Dn\Delta T + (Vn\Delta T)^2$	$p(4Dn\Delta T)^2$
Diffusion confined to a small region*	$\Lambda^2/3$	$(2\Lambda^4/15)z$
Interacting mobile proteins‡		
Short time	$4D_m n\Delta T$	$p(4D_m n\Delta T)^2$
Long time§ ($D_M < D_m$)	$4D_M n\Delta T + \Lambda^2/3$	$\sim p(4D_M n\Delta T)^2 + (2\Lambda^4/15)z$
Percolation	$\propto(m\Delta T)^x$ $(x < 1)$	ND

where

$p = [(2n^2+1)/3n(N-n+1)]$; N is the total number of positions measured; and $z = [\Lambda^2/(4ND_m\Delta T)]$

*For this example diffusion is limited to a square region of dimensions $\Lambda \times \Lambda$. Because the particle cannot exit from the defined region, $D_M = 0$, where D_M characterizes diffusion over distances $> \Lambda$.

‡For particles interacting with mobile obstacles the diffusion coefficient can be represented as varying with time or distance diffused as indicated in the text (Abney et al., 1989; Saxton, 1989). Over distances short compared to the spacing of the obstacles, their effect on diffusion is small and so the apparent diffusion coefficient, D_m, is greater than for distances large compared to the spacing over which the obstacles exert their full retarding effect to yield D_M.

§The variance for this example results from a generalization for free diffusion and diffusion in a confined region. Λ is the characteristic distance between obstacles; $\Lambda^2/4D_m$ is the correlation time for diffusion across the small domains between obstacles.

TABLE II Comparison between FPR and SPT

	Diffusion coefficient (cm^2/s)	
	FPR	SPT
Acetylcholine receptor on myofibrils	6.4×10^{-10}*	4.16×10^{-10}‡
Concanavalin *A* receptor on macrophage	4.9×10^{-10}§	3.60×10^{-11}‖

Sources *Dubinsky, et al., 1989; ‡Dubinsky, unpublished measurements; §Henis and Elson, 1981; ‖Sheetz et al., 1989.

An inherent advantage of the SPT method for cell studies is that the qualitative behavior of the particle is known before the position measurements. This is important because particles can move onto rough regions of the cell surface (e.g., microvilli or ruffles), reversibly stop diffusion (Sheetz et al., 1989), or undergo rapid forward displacements (Kucik et al., 1989; Sheetz et al., 1990). None of these phenomena would be distinguished in a normal FPR or FCS analysis but would obviously contribute to the apparent diffusion coefficient measurement. Thus, we feel that a more reliable measurement of the true membrane diffusion coefficient can be made using the SPT method.

This analysis is not limited to the study of membrane proteins. For example, it can equally be applied to the trajectories of cells undergoing chemotaxis and to the facilitated diffusion of DNA binding proteins such as lac repressor on DNA.

APPENDIX A

Relationship between $\rho(t)$ and $g_v(t)$

We consider $\{x_i | i = 0, 1, 2, \ldots, N\}$ and the corresponding velocities $\{v_i = (x_i - x_{i-1})/\Delta T | i = 1, 2, \ldots, N\}$. Therefore,

$$\begin{aligned}\langle v_n v_{n+m}\rangle &= \Sigma_n v_n v_{n+m}/N \\ &= 1/N \Sigma_n (x_n - x_{n-1})(x_{n+m} - x_{n+m-1})/(\Delta T)^2 \\ &= 1/2N \Sigma_n [-(x_n - x_{n+m})^2 - (x_{n-1} - x_{n+m-1})^2 \\ &\quad + (x_{n-1} - x_{n+m})^2 + (x_n - x_{n+m-1})^2]/(\Delta T)^2 \\ &= 1/2[-\rho_m - \rho_m + \rho_{m+1} + \rho_{m-1}]/(\Delta T)^2 \\ &= \rho_m''/2\end{aligned}$$

that is:

$$2g_v(t) = \rho''(t).$$

APPENDIX B

Variance of ρ_n

Consider the mean squared displacement of a particle diffusing in a two-dimensional plane $\xi = |r(t) - r_0|^2$ as a random variable. Its probability distribution is

$$\text{Prob}\{z \le \xi \le z + dz\} = (1/4Dt)\ \exp(-z/4Dt)dz \quad z > 0,$$

which yields $\langle\xi\rangle = 4Dt$ and, for $\Delta\xi = \xi - \langle\xi\rangle$, $\langle\Delta\xi\Delta\xi\rangle = \langle\xi\rangle^2$.

If we have K independent measurements of ξ: $\xi(1), \xi(2), \ldots, \xi(K)$, and define $\bar{\xi} = [\xi(1) + \xi(2) + \cdots + \xi(K)]/K$, then the probability distribution for $\bar{\xi}$ can be obtained as successive convolutions of Prob $\{z \le \xi \le z + dz\}$ with itself (Feller, 1957). By a recurrent inductive calculation, we have:

$$\text{Prob}\{z \le \bar{\xi} \le z + dz\} = \frac{K^K z^{K-1}}{(K-1)!}\frac{\exp(-Kz/4Dt)}{(4Dt)^K}dz \quad z > 0 \quad \text{(B1)}$$

where $t = n\Delta T$. Therefore, $\langle\bar{\xi}\rangle = \langle\xi\rangle$, $\langle\Delta\bar{\xi}\Delta\bar{\xi}\rangle = \langle\Delta\xi\Delta\xi\rangle/K = \langle\xi\rangle^2/K$, and the relative error $(\langle\Delta\bar{\xi}\Delta\bar{\xi}\rangle/\langle\bar{\xi}\rangle)^{1/2} = 1/\sqrt{K}$.

Furthermore, the probability of finding a value of the ratio $\bar{\xi}/\langle\xi\rangle$ greater than some number λ is obtained simply by integrating Eq. B1:

$$\begin{aligned}\text{Prob}\{\bar{\xi}/\langle\xi\rangle \ge \lambda\} &= \int_\lambda^{+\infty} \text{Prob}\{z \le \bar{\xi}/\langle\xi\rangle \le z + dz\}\,dz \\ &= \int_\lambda^{+\infty} K^K z^{K-1}/(K-1)!\ \exp(-Kz)\,dz \\ &= [1 + K\lambda + (K\lambda)^2/2! \\ &\quad + \cdots (K\lambda)^{K-1}/(K-1)!]e^{-K\lambda} \\ &= Q(2K\lambda|2K) \qquad \text{(B2)}\end{aligned}$$

Here $Q(\chi^2|\nu)$ is the χ^2 probability function which can be found in mathematical tables (Abramowitz and Stegun, 1964).

Now we define $\xi_1 = |r(t_2) - r(0)|^2$ and $\xi_2 = |r(t_3) - r(t_1)|^2$, $0 \le t_1 \le t_2 \le t_3$. The correlation between ξ_1 and ξ_2 can be characterized by the correlation coefficient $\langle\Delta\xi_1\Delta\xi_2\rangle/(\langle\Delta\xi_1^2\rangle\langle\Delta\xi_2^2\rangle)^{1/2}$. Because the diffusion process is Markovian:

$$\begin{aligned}&\text{Prob}\{r_0, 0; r_1, t_1; r_2, t_2; r_3, t_3\} \\ &\quad = \text{Prob}\{r_3|r_2, t_3 - t_2\} \times \text{Prob}\{r_2|r_1, t_2 - t_1\} \\ &\quad \times \text{Prob}\{r_1|r_0, t_1\} \times \text{Prob}\{r_0\}\end{aligned}$$

therefore,

$$\begin{aligned}\langle\Delta\xi_1\Delta\xi_2\rangle &= \langle(r_2 - r_1)^4\rangle - \langle(r_2 - r_1)^2\rangle^2 \\ &= [4D(t_2 - t_1)]^2 \qquad \text{(B3)}\end{aligned}$$

i.e., it is proportional to the square of the time overlap between ξ_1 and ξ_2, and

$$\langle\Delta\xi_1\Delta\xi_2\rangle/(\langle\Delta\xi_1^2\rangle\langle\Delta\xi_2^2\rangle)^{1/2} = (t_2 - t_1)^2/t_2(t_3 - t_1).$$

A positive value of the correlation coefficient indicates that ξ_1 and ξ_2 are more likely to deviate from their mean values in the same direction. Moreover, when $t_2 - t_1 = 0$, ξ_1 and ξ_2 are uncorrelated. (This is obviously also correct for $t_2 < t_1$). When $t_1 = 0$, the coefficient is equal to t_2/t_3.

When ρ_n is calculated using a time average, $\xi(1) = |r_n - r_0|^2$, $\xi(2) = |r_{n+1} - r_1|^2, \ldots, \xi(K) = |r_{n+K-1} - r_{K-1}|^2$,

$$\begin{aligned}\rho_n &= [\xi(1) + \xi(2) + \cdots + \xi(K)]/K \\ &= \left\langle \sum_{i=0}^{N-1} |r_{n+i} - r_i|^2 \right\rangle \\ &= \langle |r_{n+i} - r_i|^2\rangle + (2/N^2) \\ &\quad \sum_{i=1}^{N-1}\sum_{j=0}^{i-1} \langle |r_{n+1} - r_i|^2 |r_{n+j} - r_j|^2\rangle.\end{aligned}$$

Depending on the time interval of the measurements, these ξ's are not necessarily statistically independent. Hence, there will be a correction factor due to this consideration. A complex calculation yields:

$$(\Delta\rho_n\Delta\rho_n/\langle\rho_n\rangle)^{1/2} = \begin{cases}[(4n^2K + 2K + n - n^3)/6nK^2]^{1/2} & K \ge n \\ [1 + (K^3 - 4nK^2 + 4n - K)/6n^2K]^{1/2} & K \le n\end{cases} \quad \text{(B4)}$$

when $K \gg n$, the relative error is:

$$[\Delta\rho_n\Delta\rho_n/\langle\rho_n\rangle)^{1/2} \simeq [(2n^2 + 1)/3nK]^{1/2} \sim (2n/3K)^{1/2} \qquad \text{(B5)}$$

which is proportional to $(K/n)^{-1/2}$ rather than $K^{-1/2}$. This correction is significant, especially when n is large. When $n = 1$, $(\Delta\rho_n\Delta\rho_n/\langle\rho_n\rangle)^{1/2} = 1/\sqrt{K}$ as expected for uncorrelated ξ's.

APPENDIX C

Covariance of ρ_n and ρ_m

We consider the correlation coefficient of any two ρ_n and ρ_m.

$$\rho_n = \sum_{i=0}^{N-n} |r_{i+n} - r_i|^2/(N - n + 1)$$

$$\rho_m = \sum_{i=0}^{N-m} |r_{i+m} - r_i|^2/(N - m + 1),$$

where N is the total number of position measurements. Without loss of generality, let us assume that $m > n$. Therefore $\langle\rho_n\rangle = 4Dn\Delta T$, $\langle\rho_m\rangle = 4Dm\Delta T$, and:

$$\langle\Delta\rho_n\Delta\rho_m\rangle/[\langle(\Delta\rho_n)^2\rangle\langle(\Delta\rho_m)^2\rangle]^{1/2} \simeq n(N - m)(3 - n/m)^2/4m(N - n).$$

If $m, n \ll N$ and $m \sim n$, then:

$$\langle\Delta\rho_n\Delta\rho_m\rangle/[\langle(\Delta\rho_n)^2\rangle\langle(\Delta\rho_m)^2\rangle]^{1/2} \simeq n/m.$$

We are grateful to Drs. Jeff Gelles and Scott Kuo for critical reading of the manuscript, and to Professor Jeffrey Skolnick and Dr. Dennis Kucik for useful discussions. We would also like to thank an anonymous reviewer for a number of useful suggestions and constructive criticisms.

This work is supported by National Institutes of Health grants GM38838 to Elliot L. Elson, GM36277 and NS23345 and Muscular Dystrophy to Michael P. Sheetz.

Received for publication 23 October 1990 and in final form 29 April 1991.

REFERENCES

Abney, J. R., B. A. Scalettar, and J. C. Owicki. 1989. Self diffusion of interacting membrane proteins. *Biophys. J.* 55:817–833.

Abramowitz, M., and I. A. Stegun. 1964. Handbook of Mathematical Functions. Dover Publications, Inc., New York. 940 pp.

Angelides, K. J., W. E. Lawrence, D. J. Loftus, and E. L. Elson. 1988. Distribution and lateral mobility of voltage-dependent sodium channels in neurons. *J. Cell Biol.* 106:1911–1925.

Bretscher, M. S. 1976. Directed lipid flow in cell membranes. *Nature (Lond.).* 260:21–22.

Chandrasekhar, S. 1943. Stochastic problem in physics and astronomy. *Rev. Mod. Phys.* 15:1–89.

Chazotte, B. and C. R. Hackenbrock. 1989. Lateral diffusion as a rate-limiting step in ubiquinone mediated mitochondrial electron transport. *J. Biol. Chem.* 264:4978–4985.

Cummins, H. Z., F. D. Carlson, T. J. Herbert, and G. Woods. 1969. Translational and rotational diffusion constants of tobacco mosaic virus from Rayleigh linewidths. *Biophys. J.* 9:520–546.

Cherry, R. J. 1979. Rotational and lateral diffusion of membrane proteins. *Biochim. Biophys. Acta.* 559:289–327.

de Brabander, M., R. Nuydens, H. Geerts, and C. R. Hopkins. 1988. Dynamic behavior of the transferrin receptor followed in living epidermoid carcinoma (A431) cells with nanovid microscopy. *Cell Motil. Cytoskeleton.* 9:30–47.

Dembo, M., and A. K. Harris. 1981. Motion of particles adhering to the leading lamella of crawling cells. *J. Cell Biol.* 91:528–536.

Duband, J. L., G. H. Nuckolls, A. Ishihara, T. Hasegawa, K. M. Yamada, J. P. Thiery, and K. Jacobson. 1988. Fibronectin receptor exhibits high lateral mobility in embryonic locomoting cells but is immobile in focal contacts and fibrillar streaks in stationary cells. *J. Cell Biol.* 107:1385–1396.

Dubinsky, J. M., D. J. Loftus, G. D. Fischbach, and E. L. Elson. 1989. Formation of acetylcholine receptor clusters in chick myotubes: migration or new insertion? *J. Cell Biol.* 109:1733–1743.

Eisinger, J., J. Flores, and W. P. Petersen. 1986. A milling crowd model for local and long-range obstructed lateral diffusion. *Biophys. J.* 49:987–1001.

Elson, E. L. 1985. Fluorescence correlation spectroscopy and photobleaching recovery. *Annu. Rev. Phys. Chem.* 36:379–406.

Feller, W. 1957. An Introduction to Probability Theory and Its Applications. John Wiley and Sons, New York. 461 pp.

Geerts, H., M. De Brabander, R. Nuydens, S. Geuens, M. Moeremans, J. De Mey, and P. Hollenbeck. 1987. Nanovid tracking: a new automatic method for the study of mobility in living cells based on colloidal gold and video microscopy. *Biophys. J.* 52:775–785.

Gelles, J., B. J. Schnapp, and M. P. Sheetz. 1988. Tracking kinesin-driven movements with nanometer-scale precision. *Nature (Lond.).* 331:450–453.

Ghosh, R. N., and Webb, W. W. 1990. Evidence for intra-membrane constraints to cell surface LDL receptor motion. *Biophys. J.* 57:286*a*. (Abstr.)

Gross, D. J., and W. W. Webb. 1988. Cell surface clustering and mobility of the liganded LDL receptor measured by digital fluorescence microscopy. *In* Spectroscopic Membrane Probe. Vol II. L. M. Loew, editor. CRC Press Inc., Boca Raton, FL. 19–48.

Henis, Y. I., and E. L. Elson. 1981. Differences in the response of several cell types to inhibition of surface receptor mobility by local concanavalin A binding. *Exp. Cell Res.* 136:189–201.

Howard, J., and A. J. Hudspeth. 1987. Mechanical relaxation of the hair bundle mediates adaptation in mechanoelectrical transduction by the bullfrog's saccular hair cell. *Proc. Natl. Acad. Sci. USA.* 84:3064–3068.

Kamimura, A., and R. Kamiya. 1989. High-frequency nanometre-scale vibration in 'quiescent' flagellar axonemes. *Nature (Lond.).* 340:476–478.

Kolinski, A., J. Skolnick, and R. Yaris. 1986. On the short time dynamics of dense polymeric systems and the origin of the glass transition: a model system. *J. Chem. Phys.* 84:1922–1931.

Kucik, D. F., E. L. Elson, and M. P. Sheetz. 1989. Forward transport of glycoproteins on leading lamellipodia in locomoting cells. *Nature (Lond.).* 340:315–317.

Landau, L. D., and E. M. Lifshitz. 1969. Statistical Physics. Pergamon Press, Oxford. 484 pp.

Magde, D., W. W. Webb, and E. L. Elson. 1978. Fluorescence correlation spectroscopy. III. Uniform translation and laminar flow. *Biopolymers.* 17:361–376.

McCloskey, M. A., and M. M. Poo. 1986. Rates of membrane-associated reactions: reduction of dimensionality revised. *J. Cell Biol.* 102:88–96.

Nossal, R. 1971. Spectral analysis of laser light scattered from motile microorganisms. *Biophys. J.* 11:341–354.

Poo, M. M. 1981. In situ electrophoresis of membrane components. *Annu. Rev. Biophys. Bioeng.* 10:245–276.

Ryan, T. A., J. Myers, D. Holowka, B. Baird, and W. W. Webb. 1988. Molecular crowding on the cell surface. *Science (Wash. DC).* 239:61–64.

Saxton, M. J. 1987. Lateral diffusion in an archipelago. The effect of mobile obstacles. *Biophys. J.* 52:989–997.

Saxton, M. J. 1989. Lateral diffusion in an archipelago. Distance dependence of the diffusion coefficient. *Biophys. J.* 56:615–622.

Saxton, M. J. 1990. Lateral diffusion in a mixture of mobile and immobile particles. A Monte Carlo study. *Biophys. J.* 58:1303–1306.

Schlessinger, J. 1986. Allosteric regulation of the epidermal growth factor receptor kinase. *J. Cell Biol.* 103:2067–2072.

Sheetz, M. P. 1983. Membrane skeletal dynamics: role in modulation of red cell deformability, mobility of transmembrane proteins, and shape. *Semin. Hematol.* 20:175–188.

Sheetz, M. P., S. Turney, H. Qian, and E. L. Elson. 1989. Nanometre-level analysis demonstrates that lipid flow does not drive membrane glycoprotein movements. *Nature (Lond.).* 340:284–288.

Sheetz, M. P., N. L. Baumrind, D. B. Wayne, and A. L. Pearlman. 1990. Concentration of membrane antigens by forward transport and trapping in neuronal growth cones. *Cell.* 61:231–241.

van Zoelen, E. J. J., L. G. J. Tertoolen, and S. W. deLaat. 1983. Simple computer method for evaluation of lateral diffusion coefficients from fluorescence photobleaching recovery kinetics. *Biophys. J.* 42:103–108.

Yechiel, E., and M. Edidin. 1987. Micrometer-scale domains in fibroblast plasma membranes. *J. Cell Biol.* 105:755–760.

Zwanzig, R. 1965. Time-correlation function and transport coefficients in statistical mechanics. *Annu. Rev. Phys. Chem.* 16:67–102.